

# Sexual Attraction in the Silkworm Moth: Nature of Binding of Bombykol in Pheromone Binding Protein—An Ab Initio Study

Vojtěch Klusák,<sup>1,2</sup> Zdeněk Havlas,<sup>1,\*</sup>  
Lubomír Rulíšek,<sup>1</sup> Jiří Vondrášek,<sup>1</sup>  
and Aleš Svatoš<sup>1,3,\*</sup>

<sup>1</sup>Institute of Organic Chemistry and Biochemistry  
of the Academy of Sciences of the Czech Republic and  
Center for Complex Molecular Systems and Biomolecules  
Flemingovo nám. 2  
Praha 6, 166 10

<sup>2</sup>Charles University  
Department of Physical and Macromolecular Chemistry  
Albertov 6  
Praha 2, 128 43  
Czech Republic

<sup>3</sup>Max-Planck-Institute for Chemical Ecology  
Winzerlaer Str. 10  
D-07745 Jena  
Germany

## Summary

An analysis of the crystal structure of [BmPBP...bombykol] complex identified nine amino acid residues involved in a variety of intermolecular interactions binding the ligand. Using simple model fragments as the representatives of the residues, the interaction energies of their complexes with bombykol were calculated using high-level ab initio methods. The results were discussed in terms of the method and basis set dependence and were further corrected to account for their pair nonadditivities. This enabled us to describe quantitatively the nature and origin of the binding forces in terms of contribution of the individual amino acids and individual types of interaction to the overall stability. All of these interactions are well defined and cannot be considered as nonspecific hydrophobic interactions, one of the major conclusions of this work.

## Introduction

Interactions of insects with their surroundings are mostly based on chemical signals. One of the most remarkable communication systems known mediates sexual behavior of moths. Mature females ready to have offspring emit a sexual pheromone from their abdomen to attract conspecific males for mating. The “single-pheromone molecule” tuned detection system [1] of males is located in branches of males’ antennae. On these antennae are located olfactory hairs, *sensilla trichodea*, which are filled with sensillar lymph and house specialized dendritic cells innervated to insect brain globular structures. Here, the signal received from the cell is processed and further recognized as a call for copulation.

The sensillar lymph contains a high concentration (10 mM) of water-soluble pheromone binding protein (PBP), whose role is not fully understood. Three possible sce-

narios have been suggested [2]: (1) PBP acts as a carrier that shuffles the lipophilic pheromone through the sensillar lymph to the pheromone receptor; (2) PBP-pheromone complex is recognized by a putative receptor; and (3) PBP is involved in the pheromone “cleaning” after its recognition on the receptor.

PBPs belong to a family of odorant binding proteins (OBP), which exhibit a certain degree of functional similarity (but not sequence homology) to fatty acid binding proteins (FABP) and belong to the lipocalin family.

For sexual communication, the silkworm moth *Bombyx mori* (Lepidoptera, Bombycidae) uses sex pheromone composed of three molecular species: (10*E*,12*Z*)-hexadeca-10,12-dien-1-ol, bombykol; (10*E*,12*E*)-hexadeca-10,12-dien-1-ol; and (10*E*,12*Z*)-hexadeca-10,12-dienal [3, 4, 5]. The first component is by far the most abundant. A pheromone binding protein (BmPBP) has been isolated from male antennae and biochemically characterized [6]. The principal contributions to understanding its role were: (1) the determination of the crystal structure of its complex with the pheromone [7]; (2) evidence for the existence of this complex in solution using electrospray ionization mass spectroscopy (ESI-MS) [8, 9]; and (3) the indication of pH-dependent conformation changes that alternate the binding and/or release of the pheromone from PBP using circular dichroism (CD), fluorescence spectroscopy [10], and nuclear magnetic resonance (NMR) [11].

These studies have shown that bombykol is tightly bound in a flask-like pocket of BmPBP. The exact nature of binding is assumed unclear, except for a hydrogen bond between the polar OH group of the bombykol and the side chain of Ser56 that is quite apparent from the analysis of the crystal structure. The character of other binding interactions is rather speculative, and they are described as unspecific hydrophobic interactions. Only residues Phe12 and Phe118 are suggested to form a sandwich-like structure with the double bonds of the pheromone, but their role is also assumed to be nonspecific [7].

We attempt to give a more detailed and accurate description of the binding mode of the pheromone in the binding cavity and to examine roles of different types of interactions. We also attempt to demonstrate that it is possible to describe quantitatively all types of weak interactions, including those with a major dispersion energy component. The thorough understanding of the interactions involved in the bombykol binding can provide a solid basis for a discussion of future engineering of both molecules.

However, it must be noted that the study is dealing with a static representation of a dynamic system and that there is always a certain degree of uncertainty in the determination of the atomic positions in crystal structures owing to the thermal motion of the subunits of the studied macromolecule (quantitatively described by B factors). Besides, the X-ray crystal structures are biased during the refinement toward the minimal values of the used force field. This is especially true for low-

\*Correspondence: havlas@uochb.cas.cz (Z.H.), svatos@ice.mpg.de (A.S.)

and medium-resolution data and for heterocompounds such as a substrate.

It is assumed that both hydrophobic effect and the hydrogen bonds significantly contribute to binding of small ligands to proteins, but they differ in their specificity. While the former is considered to be nonspecific, the latter, due to its directionality, should determine the specificity of ligand-receptor binding. This simple picture recently underwent a thorough reexamination, and two important findings have been reported. First, the hydrophobic effect can be specific for a certain shape of hydrophobic (nonpolar, or low electrostatic potential) surface [12]. Second, it is becoming widely accepted that practically every amino acid, including those earlier described as hydrophobic and space filling, apparently can provide some type of attractive, orientation-specific interaction. The hydrogen bond is a complex interaction composed of several constituents that differ in their nature [13, 14]. Its understanding usually requires a partitioning of the total energy of a hydrogen bond. The various schemes for the interaction energy decomposition generally follow the one used by Morokuma [15]. Thus, we speak about it in terms of electrostatics, polarization, charge transfer, dispersion, and exchange repulsion contributions. The dispersion and exchange repulsion terms are often combined into an isotropic van der Waals contribution. Besides classical X-H...Y hydrogen bond [13, 16], amino acid side chains are capable of weaker H bonds [17–19], namely C-H...O [20], X-H... $\pi$  (X-H functional group in a weak interaction with functional group containing  $\pi$  electrons) (X = O, N, S, C) [21–23], and  $\pi$ ... $\pi$  [24–27] interactions. Then, there are interactions of hydrocarbon chains of almost purely van der Waals character which must be also taken into account. Although they are not specific with respect to C-H...C angle [28], the shape of surfaces of interacting species can be complementary (i.e., specific) [12]. The interaction energy is not negligible and is considerably dependent on their orientation [29–31].

The qualitative (or semiquantitative) energetical description of the [BmPBP-bombykol] structure can be carried out using the interaction parameters derived from statistical structural analysis (database research) or the high-level calculations of small molecular complexes. However, to account for specific distance/orientation between ligand and receptor groups and to obtain the accurate value of the interaction energy, an appropriate description of the model representing the system of interest must be applied. The resulting values can then help us to distinguish between minor changes in the structure of ligand or its two possible orientations. On the protein side, it may give us important information about effects of various mutations in the binding site or elucidate which of two side chains' orientation with equal occupancy seen in X-ray crystal structure is more favorable.

For polar molecules, it is classical electrostatics [32] that usually gives a simplified, yet sufficiently accurate description of the interaction process. Molecular mechanics—widely used for theoretical treatment of macromolecules—usually describes nonbonding interactions by the coulombic electrostatic term with the fixed point charges on the atoms and Lenard-Jones potential

for van der Waals interactions. However, for interactions where nonelectrostatic contributions prevail, it is problematic and its application is usually accompanied by comparison [33, 34] with nonempirical (ab initio) calculations or experimental results, which prohibits its usage as a routine and universal method. We believe that even a tedious and large-scale reparametrization of the empirical parameters utilizing the most recent high-level quantum chemical data will not change this situation in near future.

Nowadays, only the size-consistent correlated ab initio methods are capable of accurate description of all the above-mentioned types of weak interactions. Unfortunately, these methods are limited to complexes of rather small molecules. The most common method of choice for systems of size similar to the model intermolecular complex studied in this work is the second order Møller-Plesset (MP2) perturbation method [35]. When used together with the resolution of identity technique (RI-MP2 method) [36, 37], a very favorable “accuracy/CPU time” ratio can be achieved [38, 39].

However, MP2 method is known to overestimate the interaction energies in many cases [40–43]. These deficiencies are improved to a large extent in coupled cluster (CC) method [44, 45], incorporating single, double, and noniterative triple excitations (CCSD(T)) [46] and using a large and flexible basis set. Nevertheless, its usage is strongly limited by the size of a system, and the values of calculated interaction energies exhibit a similar basis set dependency to MP2 ones. On the other hand, the overestimation of the MP2 method (compared to CCSD(T)) shows only moderate basis set dependence [41, 42, 47, 48].

The interaction energy ( $\Delta E_{\text{int}}$ ) can then be expressed as

$$\Delta E_{\text{int}} = \Delta E_{\text{MP2}} + \Delta \text{CCSD(T)}. \quad (1)$$

In the above equation, the first term is the MP2 interaction energy computed with the largest possible basis set or extrapolated to the basis set limit. The second term (correction) is a difference between interaction energies obtained from MP2 and CCSD(T) calculated using a smaller basis set.

The total interaction energy of interconnected hydrogen bonds is not just a sum of contributions of the isolated bonds. In general, an interaction of two groups is influenced by the third one. On the basis of mutual polarization of the involved groups, it may be strengthened or weakened [13]. Hence, the total interaction energy of the cluster of any three molecules (A, B, and C) can be expressed as the sum of the pair interaction energies and the three-body interaction term:

$$\Delta E^{\text{ABC}} = \Delta E^{\text{AB}} + \Delta E^{\text{BC}} + \Delta E^{\text{AC}} + \Delta E^3. \quad (2)$$

Similarly, the total interaction energy of a weakly interacting four-body complex can be expressed as the sum of the pair interactions and the term  $\Delta E^4$ , which is the sum of four three-body terms and a four-body term. The sum of the nonpair contributions is called the cooperative effect and has to be taken into account for the correct description.

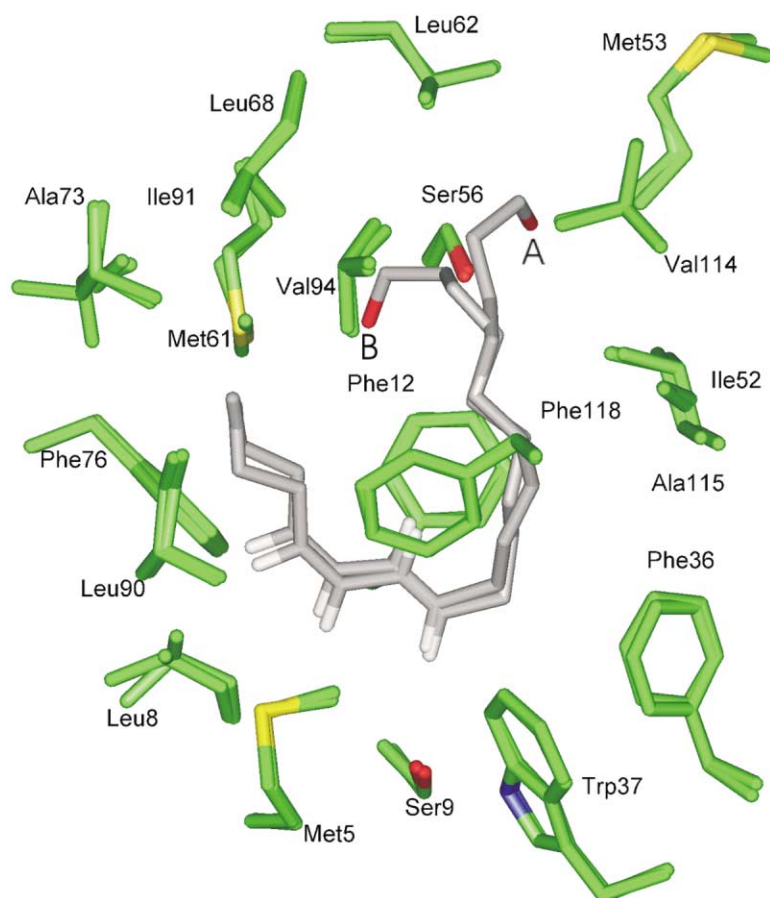


Figure 1. Schematic Representation of the Binding Cavity with Superimposed Bombykol and Amino Acid Residues from Structures A and B

Only hydrogen atoms which are connected to the bombykol double bonds are shown.

## Results and Discussion

### Analysis of X-Ray Structure and Selection of the Amino Acid Residues for Calculations

The [BmPBP...bombykol] complex consists of one protein molecule (MW 15.9 kDa) and one molecule of pheromone. Two slightly different conformations of the complex are known to build up one asymmetric unit of the crystal in solid phase [7], and hence the analysis has been performed for both structures, denoted as structures A and B throughout this work (Figure 1).

The protein consists of a single strand twisted into six  $\alpha$  helices fixed with three disulfide bonds. The four  $\alpha$  helices form a conical cavity in which the pheromone is bound. The cavity is capped by the fifth  $\alpha$  helix. There are no water molecules inside the cavity (in X-ray crystal structure).

By comparing the mean B factors of the amino acids on the surface of the binding cavity ( $19.80 \text{ \AA}^2$ ) and of the whole complex ( $25.25 \text{ \AA}^2$ ), it is apparent that the cavity of the protein is more rigid than the rest of the complex. In contrast, the pheromone molecule has a much higher mean B factor ( $40.06 \text{ \AA}^2$ ), suggesting, together with its ambiguous conformation in the binding cavity (A and B), that pheromone itself is rather flexible.

The analysis of the interactions involved in the pheromone binding according to their known parameters yielded a set of amino acids and types of interactions listed in Table 1.

The donor-acceptor (or hydrogen-acceptor) distance and the X-H-A angle are characteristic parameters of a hydrogen bond. Owing to the absence of hydrogen atom coordinates in the available X-ray crystal structure, the assessments of the angles require an additional optimization. For preliminary assessment, the donor-acceptor distances were compared to those extracted from structural or computational analyses.

(1) O-H...A or O...H-X interactions [16, 19, 49–54]. For this type of hydrogen bond, the optimum distance between nonhydrogen atoms in crystal structures range from  $2.7 \text{ \AA}$  to  $3.6 \text{ \AA}$ , depending on a type of donor and acceptor atom. Ser56 in A and Ser56 and Met61 in B fulfill this distance criterion. The distances for Ser56A and Ser56B are  $2.72 \text{ \AA}$  and  $3.10 \text{ \AA}$ , respectively, and suggest that the latter should be weaker than the former but still important. Met61 is  $3.14 \text{ \AA}$  away from the terminal oxygen of bombykol, which is indicative of another hydrogen bond. For organic molecules [19, 55] and proteins [50, 51, 55], the S-O distance between C-S-C-containing groups and O-H is  $3.37$  to  $3.53 \text{ \AA}$ . We have accounted for the possibility of S...X interaction, which is characterized by the absence of hydrogen and electrophilic character of sulfur [56], but due to character of the interacting groups and their orientation, this is not the case.

(2) C-H... $\pi$  interaction [23] is the weakest of the X-H... $\pi$  kind of interaction [17–19, 57, 58] and has the smallest electrostatic character. In the protein struc-

Table 1. Set of Selected Potential Interactions of Amino Acid Residues in BmBPB with Bombykol

Type of Interaction	Structure A			Structure B		
	AA:Atom	Bombykol-Atom	Distance (Å)	AA:Atom	Bombykol-Atom	Distance (Å)
OH...O	Ser56:O $\gamma$	O	3.10	Ser56:O $\gamma$	O	2.72
OH...S			7.58	Met61:S	O	3.14
$\pi$ , CH... $\pi$	Phe118:X	C5	4.64	Phe118:X	C6	4.32
	Phe118:X	C11	5.29	Phe118:X	C8	4.43
	Phe118:X	C14	5.06	Phe118:X	C10	5.26
$\pi$ , CH... $\pi$	Phe12:X	C8	3.98	Phe12:X	C8	4.84
	Phe12:X	C9	4.84	Phe12:X	C11	4.57
	Phe12:X	C11	4.63	Phe12:X	O	4.46
$\pi$ , CH... $\pi$	Phe36:X	C9	4.37	Phe36:X	C9	4.60
$\pi$ , CH... $\pi$	Phe76:X	C13	5.57	Phe76:X	C13	5.35
CH...O	Ser9:O $\gamma$	C10	3.70	Ser9:O $\gamma$	C10	4.00
CH... $\pi$	Leu8:C	C12	4.06	Leu8:C	C12	4.35
	Ser9:N	C12	4.36	Ser9:N	C12	4.72
Van der Waals contact	Leu8:CB	C12	3.79	Leu8:CB	C12	3.74
	Leu8:CG	C13	4.15	Leu8:CG	C13	4.16
	Leu8:CD2	C13	4.22	Leu8:CD2	C13	3.82

X represents the center of an aromatic ring, O $\gamma$  the terminal oxygen of Ser, and N and C are nitrogen and carbon atoms in the protein backbone.

tures, the distribution of the distances between C-H carbon and the center of an aromatic ring has its maximum around 3.7 Å [21]. Several aromatic residues (Phe12, Trp35, Phe36, Phe76, and Phe118) are in the vicinity of the pheromone in **A** and **B**. In particular, Phe12 and Phe118 are oriented favorably to C-H groups of the pheromone. None of C-H groups is in an ideal distance and orientation, but theoretical calculations show that the potential energy surfaces of the model systems of C-H... $\pi$  interaction are very shallow near the minimum and that substantial attraction still exists, even if intermolecular distance is larger than 4.0 Å [42]. Another C-H... $\pi$  interaction can be found between Leu8-Ser9 peptide bond and the pheromone, where peptide bond can act as an acceptor. This type of interaction has not been described in the literature, but evidence of stacking interaction of peptide bond has been reported [22]. In our case, the donor and acceptor are in favorable mutual orientation.

(3)  $\pi$ ... $\pi$  interaction: Phe12 and Phe118 are almost parallel to the plane of the conjugated double bonds of the pheromone [interplanar angle is 14° (8°) for Phe12A(B) and 20° (18°) for Phe118A(B)], while Trp35, Phe36, and Phe76 are not [58° (56°), 40° (52°), and 78° (71°), respectively]. In crystal structures of larger  $\pi$  systems with the repetitive stacking motive, the interplanar distance ranges from 3.3 Å to 3.6 Å [59]. From theoretical calculations performed for a model system of two benzene rings, it is known that the optimum distance between centers of parallel rings ranges between 3.8 and 4.1 Å, depending on the level of theory [40, 60–62]. In proteins, aromatic residues prefer to form networks of interacting aromatic side chains rather than just isolated pairs [24, 27, 63]. The distribution of distances between the ring centers has its maximum at about 5.5 Å (a set of 34 protein structures) [24]. Recently, a similar analysis has been published for minimal interatomic distance between two aromatic residues, which was found to have a maximum of 3.8 Å (a set of 593 proteins) [64].

The interaction between Phe12, Phe118, and conju-

gated double bonds of pheromone exhibit a certain degree of similarity to parallel displaced stacking of benzene dimer. The other three aromatic side chains can also contribute to binding because perpendicular or close to perpendicular orientation is favorable for the quadrupole-quadrupole interaction, an important contribution to benzene dimer interaction [47].

It must be noted that aromatic moiety can concomitantly participate in multiple interactions. It may serve as a multiacceptor site and/or partner for multiple  $\pi$ ... $\pi$  stacking [57, 65–67]. Indeed, the two amino acids Phe12 and 118 are involved to some extent in several C-H... $\pi$  interactions and a  $\pi$ ... $\pi$  stacking with the pheromone.

(4) C-H...O interactions [17, 19, 68, 69]: The separation of the groups is strongly dependent on the nature of both contact partners [70, 71, 72]. In our system, terminal OH group of Ser9 is in favorable contact with C<sub>sp2</sub>-H group of the pheromone. Although the distance is slightly larger than the mean distance found in crystal structures of organic molecules [19] and proteins [20] (both 3.5 Å), this arrangement is expected to favorably contribute to the overall interaction.

(5) Interaction of saturated hydrocarbon chains does not exhibit the directionality of a hydrogen bond [28], but still it shows orientation preference to other molecules [12, 29]. It is not surprising, then, that interaction energy of propane dimer is non-negligible, and it is considerably dependent on the mutual orientation [30, 31]. There is a close contact of this kind between Leu8 side chain and the pheromone.

We considered the previous detailed analysis as a very important step in this computational study, since it made clear that several types of interactions are present in the binding cavity. None of those, however, is in ideal conformation known from theoretical calculations on model systems, because the interacting groups belong to two separate molecules, and a balance among those interactions and geometrical constraints must be established. How are these interactions affected and which of them are strongest in effect? How strong an

impact has the multiacceptor and stacking ability of systems on the interaction energy? Are these interactions additive or is there a strong cooperativity? What is the difference in binding energy between **A** and **B**? These are questions to which the following calculations should give a clue.

#### Ab Initio Calculations of Individual Interaction Terms

Owing to computer limitations, it is not possible to carry out MP2 (RI-MP2) calculations of the entire complex to study interaction of the binding cavity with pheromone molecule. Therefore, a strategy of partitioning the whole system into well-defined, chemically distinct interacting groups has been adopted, assuming that only the nearest atoms have major influence on the strength of particular interaction. For all types of interactions selected for [BmPBP...bombykol] (Table 1), minimal models were constructed (Table 2) with the coordinates of nonhydrogen atoms fixed at the values obtained from X-ray crystal structures (both amino acid and bombykol molecule). Since all of the nearest residues of bombykol have been taken into account, this approach should describe all steric repulsion between the cavity and the ligand. It should also localize the most important attractive interactions and give an excellent opportunity to compare their strength and evaluate the different contributions in a relative scale. On the other hand, it does not yield the absolute value of interaction energy, because it is not describing a whole system and its environment. Unfortunately, the direct calculation of a binding constant ( $\Delta G$  for an entire process of pheromone desolvation and its binding to the solvated protein) is not possible nowadays by means of theoretical chemistry.

The partial molecular geometry optimization of hydrogen atoms and subsequent interaction energy calculation were performed at the RI-MP2/aug-SVP level (by RI-MP2 method in aug-SVP basis set). As the MP2 (RIMP2) method is known to overestimate the interaction energies, corrections of the RI-MP2 values were performed (see Experimental Procedures). The results are listed in Table 2.

To minimize the effects of the truncation of the system, the smaller molecules modeling the part of the protein or the pheromone were selected to capture all the important chemical properties of the real system (Experimental Procedures). If more than one amino acid residue was interacting with a part of the bombykol molecule, the cooperative effect (i.e., the pair nonadditivity in many-body interaction terms) has been also evaluated, and the values corresponding to particular interactions corrected according to Equation 2 (Table 2). However, the cooperative effect calculated separately for several systems has been shown to be negligible (in the order of 0.1%–1.4%).

The values of the interaction energies for selected amino acids in Table 3 are based on the calculated and corrected values presented in Tables 2A and 2B. The total interaction energy (the best gas-phase estimate) of bombykol molecule with BmPBP is then calculated as a sum of individual contributions.

For the purpose of this work, mapping of the cavity and relative comparison of contributions of individual

amino acids, only MP2 (RI-MP2) calculations would suffice. We expect that the importance of the correction will emerge when several X-ray structures with ligand analogs are compared. When small differences would be expected or when the error could rise by multiple summations, then the corrections would have to be estimated.

#### Types of Interactions in the PBP Binding Pocket and the Role of Hydrophobic Residues and the Hydrophobic Part of Pheromone

The difference in geometry between the two complexes (**A**, **B**) in one asymmetric unit also has an effect on the interaction energy. Besides one extra residue, Met61, interacting with the pheromone in **B** (O-S distance of 3.14 Å in **B** versus 7.58 Å in **A**), there is a shift in energy for every residue. Although these individual shifts exceed 1 kcal/mol for Ser56 ( $\Delta E_{A-B} = 1.63$  kcal/mol) and for Leu8 ( $\Delta E_{A-B} = 1.18$  kcal/mol), the total sum of contributions of all the amino acids for **A** and **B** differs only by 0.03 kcal/mol. The calculations indicate that the pheromone and the residues in the cavity are able to occupy two states with almost identical interaction energy. This is in agreement with the equal occupancies of both conformations observed in the X-ray structure. The polar terminus of the pheromone with an alcohol group shows high flexibility, as its conformations in **A** and **B** differ to a large extent. In **A**, it forms a single hydrogen bond to Ser56, while in **B** it binds both to Ser56 and to Met61, resulting in a slightly stronger interaction. Interaction energies of Phe12 and Phe118 indicate that a hybrid interaction combining multiple C-H... $\pi$  and stacking interactions is indeed present, showing that the aromatic rings can bind the pheromone with strength comparable to the “classical” H bond of the terminal OH group. The remaining aromatic moieties also contribute to the overall interaction. It is clear that together they overwhelm the contribution of the classical H bonds in [BmPBP...bombykol] complex (Figure 2) and cannot be neglected in the description. Interaction energy between OH group of Ser9 and C<sub>sp2</sub>-H group of the pheromone is attractive, indicating that a weak C-H...O hydrogen bond is also present. Interaction of pheromone with Leu8-Ser9 peptide bond also contributes to the attractive part of the overall interaction. The side chain of Leu8 exhibits a weak attraction in **A** and a weak repulsion in **B**, despite the minor difference in geometry.

For future experiments that may investigate the modification of the pheromone molecule, several observations are important. The aliphatic unsaturated hydrocarbon chain of the pheromone is responsible for dominant contribution, so its modification may be critical. Conjugated double bonds fit between aromatic rings of Phe12 and Phe118 and their modification or enlargement by addition of another double bond is expected to be problematic. A parallel displacement of stacking molecules is energetically inexpensive, but the results for Leu8 side chain show that there is simply not enough space for it. Owing to the rigidity of the cavity in comparison with the pheromone and the resting state of the protein (see analysis of **B** factors in Introduction), a reorganization of the cavity can be energetically expensive. Thus, its

Table 2. Interaction Energies of Complexes Representing Interactions of Selected Amino Acids in Table 1 with Pheromone in the Binding Cavity of BmPBP

A. Structure A			
Interaction <sup>a</sup>	Model of Interaction Calculated	$E_{MP2}^b$	$E_{cor}^c$
O,C1-4...Ser56	[Butanol...methanol]	-4.84	-4.42
O,C1...Ser56	[Methanol...methanol]	-4.57	-4.18
Bom...Phe118	[(10E,12Z)-hexadecadiene-1-ol...benzene]	-4.70	-4.29
Bom...Phe12	[(10E,12Z)-hexadecadiene-1-ol...benzene]	-4.15	-3.78
Bom...Phe36	[(10E,12Z)-hexadecadiene-1-ol...benzene]	-2.02	-1.81
Bom...Phe76	[(10E,12Z)-hexadecadiene-1-ol...benzene]	-1.41	-1.25
C8-13...Trp37... Phe36	[(1,3E)-Hexadiene...indole]	-1.38	-1.22
	[(1,3E)-Hexadiene...benzene]	-1.50	-1.33
	[Benzene...indole]	-4.22	-3.84
	$\Delta E^d = -0.05$ kcal/mol <sup>d</sup>		
C4-15...Phe12...Phe118	[(3Z,5E)-Dodecadiene...benzene12]	-4.49	-4.10
	[(3Z,5E)-Dodecadiene...benzene118]	-3.52	-3.20
	$\Delta E^d = -0.01$ kcal/mol <sup>d</sup>		
C9-14...Ser9	[(2E,4Z)-Hexadiene...methanol]	-1.04	-0.91
C9-14...Leu8Ser9 peptide	[(2E,4Z)-Hexadiene...N-methyl acetamide]	-0.98	-0.85
O,C1...Phe118	[Methanol...benzene]	0.00	0.05
C2-8...Phe118	[Heptane...benzene]	-2.12	-1.90
C9-16...Phe118	[(2E,4Z)-octadiene...benzene]	-2.65	-2.39
C5...Phe118	[Methane...benzene]	-0.82	-0.70
C4-6...Phe118	[Propane...benzene]	-1.41	-1.24
C9-16...Leu8	[(2E,4Z)-octadiene...2-methylbutane]	-0.92	-0.82
B. Structure B			
O,C1...Ser56...Met61...Phe12	[Methanol...methanol56]	-3.08	-2.79
	[Methanol...dimethyl sulfide]	-3.09	-2.80
	[Methanol...benzene]	-0.27	-0.20
	[Dimethyl sulfide...benzene]	-0.86	-0.74
	[Benzene...methanol56]	-0.80	-0.69
	[Dimethyl sulfide...methanol56]	-0.47	-0.38
	$\Delta E^d = -0.12$ kcal/mol <sup>d</sup>		
Bom...Phe118	[(10E,12Z)-hexadecadiene-1-ol...benzene]	-3.94	-3.59
Bom...Phe12	[(10E,12Z)-hexadecadiene-1-ol...benzene]	-5.01	-4.57
Bom...Phe36	[(10E,12Z)-hexadecadiene-1-ol...benzene]	-2.15	-1.93
Bom...Phe76	[(10E,12Z)-hexadecadiene-1-ol...benzene]	-1.30	-1.15
C8-13...Trp37...Phe36	[(1,3E)-Hexadiene...indole]	-1.36	-1.20
	[(1,3E)-Hexadiene...benzene]	-1.47	-1.30
	[Benzene...indole]	-4.72	-4.31
	$\Delta E^d = -0.03$ kcal/mol <sup>d</sup>		
C9-14...Ser9	[(2E,4Z)-Hexadiene...methanol]	-0.98	-0.84
C9-14...Leu8Ser9 peptide	[(2E,4Z)-Hexadiene...N-methyl acetamide]	-0.92	-0.79
C9-16...Leu8	[(2E,4Z)-octadiene...2-methylbutane]	0.30	0.36

Interaction energies are in kcal/mol.  
<sup>a</sup>Atoms of bombykol (Bom)...amino acid from BmPBP.  
<sup>b</sup>Pair interaction energy corrected for BSSE.  
<sup>c</sup>See text.  
<sup>d</sup>Many-body contributions to interaction energy (see Introduction).

Table 3. The Interaction Energy of Amino Acid Residues in BmPBP with Bombykol

Complex A <sup>a</sup>	$E_{cor}^b$ [kcal/mol]	Complex B	$E_{cor}^b$ [kcal/mol]
Ser56	-4.42	Phe12	-4.57
phe118	-4.29	phe118	-3.59
Phe12	-3.78	Met61	-2.80
Phe36	-1.81	Ser56	-2.79
Phe76	-1.25	Phe36	-1.93
Trp37	-1.22	Trp37	-1.20
Ser9	-0.91	Phe76	-1.15
Pept. bond L8-S9	-0.85	Ser9	-0.84
Leu8	-0.82	Pept. Bond L8-S9	-0.79
		Leu8	0.36
Sum	-19.35	Sum	-19.32

<sup>a</sup>The three letter code and a serial number of interacting amino acid of structure A (B).

<sup>b</sup>Corrected interaction energy of bombykol with the corresponding amino acid extracted from Table 2.

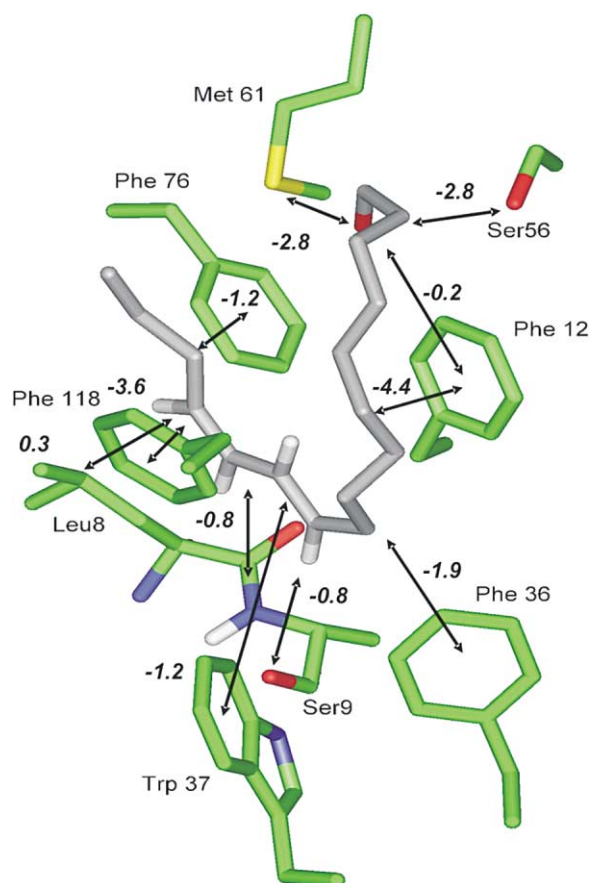


Figure 2. Schematic Representation of the Structure B Binding Cavity with Bombykol and Amino Acid Residue Side Chains  
The arrows show the main interactions of the pheromone in the binding pocket. Interaction energies are in kcal/mol.

shape may be critical for the selectivity, and the nature of interacting residues will influence the overall affinity. It is in agreement with the sequence analysis of the cavity amino acids presented by Sandler et al. [7], which revealed that the aromatic residues of the cavity are conserved in all lepidopteran OBPs. Those amino acid residues in the cavity that show no interaction and only form

the shape of the cavity are variable across lepidopteran OBPs and hence specific for BmPBP binding cavity. Since  $\text{CH}\cdots\pi$  interactions are relatively distance tolerant [42] and the CH groups of pheromone are farther-than-optimum distance from the aromatic rings, we believe that modifications in the saturated part of the pheromone increasing donor potential of the pheromone in  $\text{C-H}\cdots\pi$  interaction are possible. This may be achieved either by a polarization of C-H bonds that would increase their donor potency or by the closure of the hook shape of the pheromone using a short hydrocarbon bridge that would introduce more donors for the interaction into the cavity. For the polar end of the pheromone, two things are important: flexibility, allowing it to adopt different conformations in A and B, and the ability to concomitantly act as a donor and acceptor (this feature is mainly apparent in structure B).

### Significance

We present high-level *ab initio* calculations addressing questions about the origin of intermolecular forces that bind the pheromone inside the PBP pocket. For the first time, we were able to localize and quantitatively evaluate forces responsible for an interaction of lipophilic ligand with protein residues at such a high level of theory. In this study, it was shown that the pheromone molecule is not just expelled into the binding cavity from the outer environment (polar sensillar liquor) due to its hydrophobicity. On the contrary, the pheromone is mainly attracted by several aromatic residues in the cavity that interact (via  $\text{X-H}\cdots\pi$  and  $\pi\cdots\pi$  interactions) with practically the whole hydrocarbon unsaturated chain of the pheromone.

We would like to point out that the common analyses of ligand-receptor interactions using classical force fields are not sufficient for the accurate description of such phenomena as  $\text{C-H}\cdots\pi$  and  $\pi\cdots\pi$  interactions. The type of analysis presented here cannot be used for the calculations of the overall affinity ( $\Delta G$ ), because it does not describe the whole complex in its environment as a dynamic system. However, it yields the relative importance of the different contributions to overall binding. Thus, we consider the presented result as invaluable for an understanding of a large area of li-

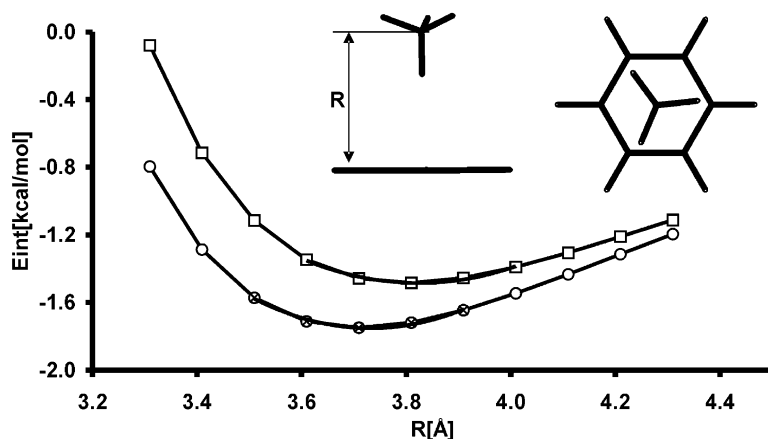


Figure 3. [Benzene...Methane] MP2/aug-SVP and MP2/aug-TZVPP Interaction Energy

Benzene...methane interaction energy, corrected for BSSE, was calculated at the MP2 level as a function of distance, R, defined in the schematic picture of the complex geometry. The curve marked by open squares is the result obtained with the aug-SVP basis set. The one marked with open circles represents values computed with larger aug-TZVPP basis set. Polynomial fit, depicted by the solid line, was used for searching the minima on the curves. They were located at 3.82 Å and 3.73 Å with the corresponding energies -1.56 kcal/mol and -1.75 kcal/mol.

Table 4. Interaction Energies of Weakly Bonded Complexes Representing All Types of Studied Interactions in [BmPBP...Bombykol] Complex

	$E_{\text{int}}$ [kcal/mol]			
	MP2 <sup>a</sup>	$\Delta\text{CCSD(T)}^b$	RI-MP2 <sup>c</sup>	CCSD(T) <sup>d,e</sup>
[Methane...benzene]	-0.51	0.10	-0.82	-0.72
[Methanol...benzene]	0.28	0.05	-0.25	-0.20
[Propane...benzene]	-0.92	0.19	-1.41	-1.22
[Butadiene...benzene]	-0.98	0.19	-1.50	-1.31
[Hexadiene...methanol]	-0.62	0.05	-1.04	-0.99
[Butadiene...N-methyl acetamide]	-0.27	0.11	-0.93	-0.82
[Methanol...dimethyl sulfide]	-1.62	0.51	-3.07	-2.55
[Butanol...methanol]	-3.50	0.29	-4.84	-4.55

<sup>a</sup> Calculated using cc-pVDZ basis set.<sup>b</sup> Difference of MP2 and CCSD(T) interaction (cc-pVDZ).<sup>c</sup> RI-MP2/aug-SVP.<sup>d</sup> Estimated CCSD(T) energy (RI-MP2 +  $\Delta\text{CCSD(T)}$ ) according to Equation 1).<sup>e</sup> Plotting RI-MP2 versus estimated CCSD(T)/aug-SVP data yielded the linear regression equation:  $y = 0.9237x + 0.0554$ ; with RMSD = 0.0096.

gand-protein interactions mediating a chemical communication by semiochemicals (alarm signals, cuticular hydrocarbon signatures, etc.), which are quite often hydrocarbons or fatty acids. The theoretical treatment of similar types of interactions as presented in this work for the PBP-pheromone complex has broad applications in related lipocaline-fatty acid complexes as well as in the general understanding of interactions of lipophilic moieties of drugs with their receptor or transport proteins.

## Experimental Procedures

### Used Methods, Basis Sets, and Programs

All the calculations were performed using Turbomole 5.3 [73] and MOLPRO 2000 [74] program suites. Several types of basis sets have been used throughout the calculations: aug-SVP, aug-TZVPP [38], and cc-pVDZ [75, 76]. Electron correlation energies were accounted for by the second-order Møller-Plesset perturbation method (MP2) [35] using approximate resolution of the identity MP2 technique (RI-MP2) [36, 37] and by coupled cluster method using single, double, and noniterative triple excitations (CCSD(T)) [46]. The values of interaction energies have been corrected for the basis set superposition error (BSSE) using the counterpoise method of Boys and Bernardi [77]. Since the crystal structure contained only nonhydrogen atoms, these were added with the standard geometrical parameters (according to geometry, atom type, and hybridization) to both bombykol and interacting amino acid residues, and their positions were optimized at the RI-MP2/aug-SVP level.

### Basis Set Dependence of the Interaction Energies

To evaluate the dependence of the results on the size (quality) of the basis set, we compared the results obtained using aug-SVP and aug-TZVPP basis sets.

A complex of benzene and methane served as a model of C-H... $\pi$  interaction. MP2/aug-SVP and MP2/aug-TZVPP interaction energies were calculated as a function of distance between benzene and methane (Figure 3). Five points around the minimum, separated by 0.1 Å, were fitted by a polynomial of the second order. The interaction energies are -1.54 kcal/mol for RI-MP2/aug-SVP and -1.75 kcal/mol for RI-MP2/aug-TZVPP. Thus, aug-SVP basis set underestimates the value of the interaction energy by 11% in comparison with aug-TZVPP basis set. For classical hydrogen bond and for stacking interaction, the former (smaller) basis set underestimates the interaction energies by 7.1% and 6.8%, respectively, in comparison with the larger basis set [38]. It shows that combination RI-MP2/aug-SVP captures most of the interaction energy and is sufficiently accurate for the quantitative comparison of different types of interaction.

### Estimation of the Errors Caused by Molecule Truncation

Errors caused by a truncation of the bombykol molecule and the amino acid residues in BmPBP were estimated at the RI-MP2/aug-SVP level. For a representative comparison, OH...O and CH... $\pi$  interactions were chosen. The truncation of the complex [butanol...methanol] (Table 2A, O,C1-4...Ser56) to [methanol...methanol] (Table 2A, O,C1...Ser56) decreases the interaction energy by 5.6%, as can be expected in gas-phase calculations (positive induction effect of propyl group). In reference [41], MP2 interaction energy extrapolated to the basis set limit of complex [water...methanol] is -4.99 kcal/mol, which is 10.6% less than complex [methanol...methanol]. In reference [42], the MP2 interaction energy extrapolated to the basis set limit of complex [methane...benzene] is -1.74 kcal/mol, which is 25.3% less than for complex [ethane...benzene]. In this study, reduction of complex [propane...benzene] (Table 2A, C4-6...Phe118) to complex [methane...benzene] (Table 2A, C5...Phe118) decreases the interaction energy by 41.8%, indicating that truncation of bonded environment has a strong impact on calculated interaction energy, especially for the C-H... $\pi$  interaction. It was an important criterion in our selection of model systems for the calculations of interaction energies (Table 2). For example, the whole pheromone molecule has been used for calculation of the interaction energy with aromatic benzene rings of the phenylalanine residues.

### Correction of MP2 Calculated Interaction Energies

The anticipated systematic errors of MP2 method (overestimation of the studied types of interactions) have been corrected by CCSD(T) method. The cc-pVDZ basis set has been used because it has been found to yield results of sufficient accuracy [42]. Owing to the huge computational demands of this method, a set of simplified complexes representing the studied structures and interactions has been selected. The results are summarized in Table 4. In this case, MP2 method systematically overestimates interaction energies by 4.8%–16.6%. The linear regression of the calculated data, RI-MP2 ( $x$  axis) versus CCSD(T) ( $y$  axis), resulted in the following equation:  $y = 0.9237x + 0.0554$ ; RMSD = 0.0096. It has been used for a calibration of RI-MP2 values, thus yielding the estimates of CCSD(T)/aug-SVP interaction energies (Table 2,  $E_{\text{cor}}$ ).

### Evaluation of the Cooperative Effect

Three complexes were selected for evaluation of the significance of the cooperative effect. First, there is an alcohol group of the pheromone in close contact with three amino acids in structure B: Ser56, Met61, and Phe12 (Table 2B, O, C1...Ser56...Met61...Phe12). Second, Phe36, Trp37, and the hydrocarbon chain of the pheromone are in close contact in both structures A and B (Table 2A, C8-13...Trp37...Phe36; Table 2B, C8-13...Trp37...Phe36). As can be seen, the cooperative effect accounts for only 1.4%, 0.7%, and 0.4% of the interaction energy, respectively. Third, the conjugated double bonds of the pheromone are sandwiched by Phe12 and



Phe118 (Table 2A, C4-15...Phe12...Phe118). The cooperative effect accounts for 0.1% of the interaction energy. It can be concluded that the neglect of the cooperative effect for the types of interactions studied in this work is a plausible approximation.

#### Acknowledgments

This work has been supported by the project LN 00A032 from the Ministry of Education of the Czech Republic (MŠMT) and completed within the framework of research project Z4 055 905. Thanks go to J.C. Clardy for providing us with X-ray coordinates data before they were made available in public databases.

Received: November 19, 2002

Revised: March 17, 2003

Accepted: March 18, 2003

Published: April 21, 2003

#### References

1. Kaissling, K.E., and Priesner, E. (1970). Smell threshold of the silkworm. *Naturwissenschaften* 57, 23–28.
2. Kaissling, K.E. (2001). Olfactory perireceptor and receptor events in moths: A kinetic model. *Chem. Senses* 26, 125–150.
3. Butenandt, A., Beckmann, R., Stamm, D., and Hevker, E. (1959). On the sex pheromone of the silkworm moth *Bombyx mori*. Isolation and structure. *Z. Naturforsch.* B 14, 283–284.
4. Kasang, G., Kaissling, K.E., Vostrowsky, O., and Bestmann, J. (1978). Bombykal the second component of the *Bombyx mori* L. silkworm pheromone. *Angew. Chem.* 90, 74–75.
5. Kasang, G., Schneider, D., and Schäfer, W. (1978). The silkworm moth *Bombyx mori*. Presence of the (*E,E*)-Stereoisomer of Bombykol in the female pheromone gland. *Naturwissenschaften* 65, 337–338.
6. Maida, R., Steinbrecht, A., Ziegelberger, G., and Pelosi, P. (1993). The pheromone binding protein of *Bombyx mori*: purification, characterization and immunocytochemical localization. *Insect Biochem. Mol. Biol.* 23, 243–253.
7. Sandler, B.H., Nikonova, L., Leal, W.S., and Clardy, J. (2000). Sexual attraction in the silkworm moth: structure of the pheromone-binding-protein-bombykol complex. *Chem. Biol.* 7, 143–151.
8. Oldham, N.J., Krieger, J., Breer, H., Fishedick, A., Hoskovec, M., and Svatoš, A. (2000). Analysis of the silkworm moth pheromone binding protein-pheromone complex by electrospray-ionization mass spectrometry. *Angew. Chem. Int. Ed. Engl.* 39, 4341–4343.
9. Oldham, N.J., Krieger, J., Breer, H., Fishedick, A., Hoskovec, M., and Svatoš, A. (2001). Detection and removal of an artefact fatty acid from the binding site of recombinant Bombyx mori pheromone-binding protein. *Chem. Senses* 26, 529–531.
10. Wojtasek, H., and Leal, S.W. (1999). Conformational change in the pheromone-binding protein from *Bombyx mori* induced by pH and by interaction with membranes. *J. Biol. Chem.* 274, 30950–30956.
11. Horst, R., Damberger, F., Luginbuhl, P., Guntert, P., Peng, G., Nikonova, L., Leal, W.S., and Wuthrich, K. (2001). NMR structure reveals intramolecular regulation mechanism for pheromone binding and release. *Proc. Natl. Acad. Sci. USA* 98, 14374–14379.
12. Davis, A.M., and Teague, S.J. (1999). Hydrogen bonding, hydrophobic interaction, and failure of the rigid receptor hypothesis. *Angew. Chem. Int. Ed. Engl.* 38, 737–749.
13. Jeffrey, G.A. (1997). *An Introduction to Hydrogen Bonding*. (New York: Oxford University Press).
14. Scheiner, S. (1997). *Hydrogen Bonding. A Theoretical Perspective*. (New York: Oxford University Press).
15. Morokuma, K. (1977). Why do molecules interact? The origin of electron donor-acceptor complexes, hydrogen bonding and proton affinity. *Acc. Chem. Res.* 10, 294–300.
16. Jeffrey, G.A., and Saenger, W. (1991). *Hydrogen Bonding in Biological Structures*. (Berlin: Springer-Verlag).
17. Desiraju, G.R., and Steiner, T. (1999). *The Weak Hydrogen Bond in Structural Chemistry and Biology*. (New York: Oxford University Press).
18. Desiraju, G.R. (2002). Hydrogen bridges in crystal engineering: interactions without borders. *Acc. Chem. Res.* 35, 565–573.
19. Steiner, T. (2002). The hydrogen bond in the solid state. *Angew. Chem. Int. Ed. Engl.* 41, 48–76.
20. Derewenda, Z.S., Lee, L., and Derewenda, U. (1995). The occurrence of C-H...O hydrogen bonds in proteins. *J. Mol. Biol.* 252, 248–262.
21. Brandl, M., Weiss, M.S., Jabs, A., Sühnel, J., and Hilgenfeld, R. (2001). C-H... $\pi$ -Interactions in proteins. *J. Mol. Biol.* 307, 357–377.
22. Steiner, T., and Koellner, G. (2001). Hydrogen bonds with  $\pi$ -acceptors in proteins: Frequencies and role in stabilizing local 3D structures. *J. Mol. Biol.* 305, 535–557.
23. Nishio, M., Hirota, M., and Umezawa, Y. (1998). *The CH/ $\pi$  Interaction: Evidence, Nature, and Consequences*. (New York: John Wiley & Sons).
24. Burley, S.K., and Petsko, G.A. (1985). Aromatic-aromatic interaction: A mechanism of protein structure stabilisation. *Science* 229, 23–28.
25. Singh, J., and Thornton, J.M. (1985). The interaction between phenylalanine rings in proteins. *FEBS Lett.* 191, 1–6.
26. Mitchell, J.B.O., Nandi, C.L., McDonald, I.K., Thornton, J.M., and Price, S.L. (1994). Amino/aromatic interactions in proteins: Is the evidence stacked against hydrogen bonding? *J. Mol. Biol.* 239, 315–331.
27. Baldwin, R.L. (2002). Making a network of hydrophobic clusters. *Science* 295, 1957–1958.
28. Steiner, T., and Desiraju, G.R. (1998). Distinction between the weak hydrogen bond and the van der Waals interaction. *Chem. Commun.* 891–892.
29. Cole, J.C., Robin, T., and Verdonk, M.L. (1998). Directional preferences of intermolecular contacts to hydrophobic groups. *Acta Crystallogr. D* 54, 1183–1193.
30. Tsuzuki, S., Uchimaru, T., Mikami, M., and Tanabe, K. (2002). High level ab initio calculation of intermolecular of propane dimer: Orientation dependence of interaction energy. *J. Phys. Chem. A* 106, 3867–3872.
31. Jalkanen, J.P., Mahlanen, R., Pakkanen, T.A., and Rowley, L.R. (2002). Ab initio potential energy surfaces of the propane dimer. *J. Chem. Phys.* 116, 1303–1312.
32. Szabó, G.N., and Ferenczy, G.G. (1995). Molecular electrostatics. *Chem. Rev.* 95, 829–847.
33. Hobza, P., Kabeláč, M., Šponer, J., Mejzlík, P., and Vondrášek, J. (1997). Performance of empirical potentials (AMBER, CFF95, CVFF, CHARMM, OPLS, POLTEV), semiempirical quantum chemical methods (AM1, MNDO/M, PM3), and ab initio Hartree-Fock method for interaction of DNA bases: Comparison with nonempirical beyond Hartree-Fock results. *J. Comput. Chem.* 18, 1136–1150.
34. Řeha, D., Kabeláč, M., Ryjáček, F., Šponer, J., Šponer, J.E., Elstner, M., Šuhaj, S., and Hobza, P. (2002). Intercalators. 1. Nature of stacking interactions between intercalators (ethidium, daunomycin, ellipticine, and 4',6'-diaminide-2-phenylindole) and DNA base pairs. Ab initio quantum chemical, density functional theory, and empirical potential study. *J. Am. Chem. Soc.* 124, 3366–3376.
35. Møller, C., and Plesset, M.S. (1934). Note on an approximation treatment for many-electron systems. *Phys. Rev.* 46, 618–622.
36. Feyereisen, M., Fitzgerald, G., and Komornicki, A. (1993). Use of approximate integrals in ab initio theory — an application in MP2 energy calculations. *Chem. Phys. Lett.* 208, 359–363.
37. Vahtras, O., Almlöf, J., and Feyereisen, M.W. (1993). Integral approximations for LCAO-SCF calculation. *Chem. Phys. Lett.* 213, 514–518.
38. Jurečka, P., Nachtigall, P., and Hobza, P. (2001). RI-MP2 calculation with extended basis sets — promising tool for study of H-bonded and stacked DNA base pairs. *Phys. Chem. Chem. Phys.* 3, 4578–4582.
39. Hobza, P., and Šponer, J. (2002). Toward true DNA base-stacking energies: MP2, CCSD(T), and complete basis set calculations. *J. Am. Chem. Soc.* 124, 11802–11808.
40. Hobza, P., Selzle, H.L., and Schlag, E.W. (1996). Potential energy

- surface for the benzene dimer. Results of ab initio CCSD(T) calculations show two nearly isoenergetic structures: T-shaped and parallel-displaced. *J. Phys. Chem.* **100**, 18790–18794.
41. Tsuzuki, S., Uchimaru, T., Matsumara, K., Mikami, M., and Tanabe, K. (1999). Effects of basis set and electron correlation on the calculated interaction energies of hydrogen bonding complexes: MP2/cc-pVD5Z calculations of H<sub>2</sub>O-MeOH, H<sub>2</sub>O-Me<sub>2</sub>O, H<sub>2</sub>O-H<sub>2</sub>CO, MeOH-MeOH and HCOOH-HCOOH complexes. *J. Chem. Phys.* **110**, 11906–11910.
  42. Tsuzuki, S., Honda, K., Uchimaru, T., Mikami, M., and Tanabe, K. (2000). The magnitude of the CH/π interactions between benzene and some model hydrocarbons. *J. Am. Chem. Soc.* **122**, 3746–3753.
  43. Leininger, M.L., Nielsen, I.M.B., Colvin, M.E., and Janssen, C.L. (2002). Accurate structures and binding energies for stacked uracil dimers. *J. Phys. Chem. A* **106**, 3850–3854.
  44. Čížek, J. (1966). On the correlation problem in atomic and molecular systems. Calculation of wavefunction component in Ursell-type expansions using quantum-field theoretical method. *J. Chem. Phys.* **45**, 4256–4266.
  45. Čížek, J. (1969). On the use of cluster expansion and the technique of diagrams in calculations of correlation effects in atoms and molecules. *Adv. Chem. Phys.* **14**, 35–89.
  46. Raghavachari, K., Trucks, G.W., Pople, J.A., and Head-Gordon, M. (1989). A fifth-order perturbation comparison of electron correlation theories. *Chem. Phys. Lett.* **157**, 479–483.
  47. Tsuzuki, S., Honda, K., Uchimaru, T., Mikami, M., and Tanabe, K. (2002). Origin of attraction and directionality of the π/π interaction: Model chemistry calculations of benzene dimer interaction. *J. Am. Chem. Soc.* **124**, 104–112.
  48. Jurečka, P., and Hobza, P. (2002). On the convergence of the ( $\Delta E^{\text{CCSD(T)}} - \Delta E^{\text{MP2}}$ ) term for complexes with multiple H-bonds. *Chem. Phys. Lett.* **365**, 89–94.
  49. Baker, E.N., and Hubbard, R.E. (1984). Hydrogen bonding in globular proteins. *Prog. Biophys. Mol. Biol.* **44**, 97–179.
  50. Ippolito, J.A., Alexander, R.S., and Christianson, D.W. (1990). Hydrogen bond stereochemistry in protein structure and function. *J. Mol. Biol.* **215**, 457–471.
  51. Gregoret, L.M., Rader, S.D., Fletterick, R.J., and Cohen, F.E. (1991). Hydrogen bonds involving sulfur atoms in proteins. *Proteins* **9**, 99–107.
  52. Stickley, D.F., Presta, L.G., Dill, K.A., and Rose, G.D. (1992). Hydrogen bonding in globular proteins. *J. Mol. Biol.* **226**, 1143–1159.
  53. McDonald, I.A., and Thornton, J.M. (1994). Satisfying hydrogen-bonding potential in proteins. *J. Mol. Biol.* **238**, 777–793.
  54. Torshin, I.Y., Weber, I.T., and Harrison, R.W. (2002). Geometric criteria of hydrogen bonds in proteins and identification of 'bifurcated' hydrogen bonds. *Protein Eng.* **15**, 359–363.
  55. Allen, F.H., Bird, C.M., Rowland, R.S., and Raithby, P.R. (1997). Hydrogen-bond acceptor and donor properties of divalent sulphur (Y-S-Z and R-S-H). *Acta Crystallogr. B* **53**, 696–701.
  56. Pal, D., and Chakrabarti, P. (2001). Non-hydrogen bond interactions involving the methionine sulphur atom. *J. Biomol. Struct. Dyn.* **19**, 115–128.
  57. Ciunik, Z., and Desiraju, G.R. (2001). Area correction of multi-atom-acceptor hydrogen bond frequency distributions. *Chem. Commun.* **8**, 703–704.
  58. Takahashi, O., Kohno, Y., Iwasaki, S., Saito, K., Iwaoka, M., Tomoda, S., Umezawa, Y., Tsuboyama, S., and Nishio, M. (2001). Hydrogen-bond-like nature of the CH/π interaction as evidenced by crystallographic database analyses and ab initio molecular orbital calculations. *Bull. Chem. Soc. Jpn.* **74**, 2421–2430.
  59. Dahl, T. (1994). The nature of stacking interactions between organic-molecules elucidated by analysis of crystal-structures. *Acta Chem. Scand.* **48**, 95–106.
  60. Sinnokrot, M.O., Valeev, E.F., and Sherrill, C.D. (2002). Estimates of the ab initio limit for π-π interactions: The benzene dimer. *J. Am. Chem. Soc.* **124**, 10887–10893.
  61. Tsuzuki, S., Uchimaru, T., Matsumura, K., Mikami, M., and Tanabe, K. (2000). Effects of the higher electron correlation correction on the calculated intermolecular interaction energies of benzene and naphthalene dimers: comparison between MP2 and CCSD(T) calculations. *Chem. Phys. Lett.* **319**, 547–554.
  62. Jaffe, R.L., and Smith, G.D. (1996). A quantum chemistry study of benzene dimer. *J. Chem. Phys.* **105**, 2780–2788.
  63. Thomas, A., Meurisse, R., and Brasseur, R. (2002). Aromatic side-chain interactions in proteins. II. Near- and far-sequence Phe-X pairs. *Proteins* **48**, 635–644.
  64. Thomas, A., Meurisse, R., Charlotiaux, B., and Brasseur, R. (2002). Aromatic side-chain interactions in proteins. I. Main structural features. *Proteins* **48**, 628–634.
  65. Ciunik, Z., Berski, S., Katanka, Z., and Leszczynski, J. (1998). New aspects of weak C-H...π bonds: intermolecular interactions between alicyclic and aromatic rings in crystals of small compounds, peptides and proteins. *J. Mol. Struct.* **442**, 125–134.
  66. Ciunik, Z., and Jarosz, S. (1998). Hybrid interactions (stacking plus H-bonds) between molecules bearing benzyl groups. *J. Mol. Struct.* **442**, 115–119.
  67. Paul, P.K.C. (2002). Aromatic ring-aliphatic ring stacking in organic crystal structures. *Cyst. Eng.* **5**, 3–8.
  68. Wahl, M.C., and Sundaralingam, M. (1997). C-H...O hydrogen bonding in biology. *Trends Biochem. Sci.* **22**, 97–102.
  69. Jiang, L., and Lai, L.H. (2002). CH...O hydrogen bonds at protein-protein interfaces. *J. Biol. Chem.* **277**, 37732–37740.
  70. Steiner, T. (1998). Donor and acceptor strengths in C-H...O hydrogen bonds quantified from crystallographic data of small solvent molecules. *New J. Chem.* **22**, 1099–1103.
  71. Scheiner, S., Kar, T., and Pattanayak, J. (2002). Comparison of various types of hydrogen bonds involving aromatic amino acids. *J. Am. Chem. Soc.* **124**, 13257–13264.
  72. Scheiner, S., Grabowski, S.J., and Kar, T. (2001). Influence of hybridization and substitution on the properties of the CH...O hydrogen bond. *J. Phys. Chem. A* **105**, 10607–10612.
  73. Ahlrichs, R., Bär, M., Häser, M., Horn, H., and Kölmel, C. (1989). Electronic structure calculations on workstation computers: the program system TURBOMOLE. *Chem. Phys. Lett.* **162**, 165–169.
  74. Amos, R.D., Bernhardsson, A., Berning, A., Celani, P., Cooper, D.L., Deegan, M.J.O., Dobbyn, A.J., Eckert, F., Hampel, C., Hetzer, G., et al. (2002). MOLPRO, a package of ab initio programs designed by H.J. Werner and P.J. Knowles, version 2002.1. Birmingham, UK.
  75. Dunning, T.H. (1989). Gaussian-basis sets for use in correlated molecular calculations. 1. the atoms boron through neon and hydrogen. *J. Chem. Phys.* **90**, 1007–1023.
  76. Woon, D.E., and Dunning, T.H. (1993). Gaussian-basis sets for use in correlated molecular calculations. 3. the atoms aluminum through argon. *J. Chem. Phys.* **98**, 1358–1371.
  77. Boys, S., and Bernardi, F. (1970). The calculation of small molecular interactions by the differences of separate total energies: some procedures with reduced errors. *Mol. Phys.* **19**, 553–557.